Nanoscale

COMMUNICATION

View Article Online
View Journal | View Issue

Cite this: *Nanoscale*, 2014, **6**, 9415

Received 12th September 2013
Accepted 2nd October 2013

DOI: 10.1039/c3nr04760a

www.rsc.org/nanoscale

Template electrosynthesis of tailored-made helical nanoswimmers†

Jinxing Li, Sirilak Sattayasamitsathit, Renfeng Dong, Wei Gao, Ryan Tam, Xiaomiao Feng, Stephen Ai and Joseph Wang*

We demonstrate a template electrosynthesis for large-scale low-cost preparation of remarkably small magnetically driven tailored-made helical nanoswimmers that display efficient propulsion behavior and hold considerable promise for future miniature devices in the human body.

The synthesis of nanoscale structures capable of moving in liquids represents a major nanotechnological challenge.[1–6] Significant progress has been made recently towards the fabrication of micro/nanomotors that rely on local chemical fuel[7–9] or on external electrical,[10,11] optical,[12] ultrasound[13,14] and magnetic[15–19] stimuli. Among the different types of micro/nanomotors, magnetically actuated ones are extremely promising for diverse *in vivo* biomedical applications owing to their attractive swimming performance.[1,17,19] In particular, helical magnetic micro/nanoswimmers – inspired by bacterial flagellum propulsion[20] – transform a rotation around their helical axis into a translation along the helical axis to offer an efficient locomotion behavior.[17,19] However, till recently the large-scale preparation of helical micro/nanostructures has been challenging, since traditional microfabrication techniques – based on the deposition or removal of thin layers of material – have not been compatible with the preparation of complex three-dimensional (3D) helical micro/nanostructures.[19] The challenges of fabricating 3D helical swimmers have been discussed.[17,19] Several fabrication methods have been proposed recently for addressing these challenges and preparing magnetically actuated helical micro/nanoswimmers.[1,17,19] The first magnetically driven helical corkscrew-shaped microrobot (2–3 μm in diameter, 30–50 μm long) was fabricated by a self-scrolling technique that combines "top-down" lithographic patterning and a "self-organizing" step.[16,21] Even smaller highly densed helical nano-propellers were prepared in 2009 by glancing angle deposition (GLAD).[22] An attractive top-down 3D laser direct writing (DLW) of magnetic helical micromachines was demonstrated recently by Nelson's group.[23,24] Yet, these routes for fabricating helical micro/nanoswimmers require specialized and expensive instrumentation, and the dimensions of these helical magnetic motors are commonly limited by the resolution of optical lithography.

This article describes an effective and simple template electrodeposition approach for the large-scale preparation of extremely small and highly efficient helical magnetic swimmers. For over two decades, template electrosynthesis has been shown to be an attractive approach for the mass production of diverse nanostructures and nanodevices.[25] Such template-assisted electrochemical growth of different nanostructures involves electrodeposition of different materials into the cylindrical nanopores of a host porous membrane template, followed by dissolution of the template.[26,27] The versatility of the template-directed electrodeposition has been shown to be extremely useful for preparing chemically powered nanomotors, including catalytic bi-segment (Pt–Au) nanowires[27,28] and microtubular engines.[8,27,29,30] Template electrosynthesis has been used also for preparing flexible nanowire swimmers,[18] but not for fabricating helical (corkscrew-shaped) magnetic swimmers. Several groups have demonstrated recently the successful template fabrication and assembly of helical composite mesostructures.[31,32] In particular, Park's group described the synthesis of palladium (Pd) nanosprings using anodized aluminum oxide (AAO) templates and electrochemical deposition.[32]

Taking advantage of these recent advances in the electrosynthesis of nanosprings, we demonstrate in the following sections that this templating route can lead to the large-scale low-cost preparation of remarkably small magnetically driven helical nanoswimmers (down to 100 nm in diameter and 600 nm in length) that display efficient propulsion behavior. Our study demonstrates that such template synthesis provides convenient control the dimensions, geometry and composition of the helical swimmers, as desired for optimizing the

Department of Nanoengineering, University of California, La Jolla, San Diego, California 92093, USA. E-mail: josephwang@ucsd.edu

† Electronic supplementary information (ESI) available. See DOI: 10.1039/c3nr04760a

swimming performance. Geometrically tunable helical nanostructures – with varied diameter, length and spiral pitch – can be readily fabricated *via* judicious selection of the membrane template pore size, composition of the plating solution and electrodeposition parameters. Thousands of helical nanoswimmers can thus be prepared within few hours. The nanoscale dimensions and efficient propulsion behavior of these template-prepared helical nanoswimmers make them ideal candidates for future miniature devices in the human body.

As illustrated in Fig. 1, the new protocol for fabricating helical nanoswimmers is based on the procedure described by Park and coworkers[32] for creating Pd nanosprings. The preparation of such Pd nanohelices relies on electrochemical co-deposition of Pd^{2+} and Cu^{2+} inside the nanoscopic pores of AAO membrane templates using an acidic environment. Gold nanorods (~1 μm long) were electrodeposited initially within the nanopores to form a uniform solid base essential for the growth of the Pd/Cu nanorods (Fig. 1a). Subsequently, a solution containing 30 mM $PdCl_2$, 20 mM $CuCl_2$, and 0.1 M HCl was used for growing the Pd/Cu nanorods (Fig. 1b). An OH group terminated Al_2O_3 surface and the H^+ in acidic solution, along with a suitable reduction potential, are essential for the effective reduction of Pd^{2+} (during the co-deposition with Cu) to form crystal structures on the nanopore wall.[32] Dissolution of the membrane template (Fig. 1c) and etching of copper from the nanorod (Fig. 1d) result in Pd nanohelices. Subsequent electron beam evaporation of a nanometer-thick magnetic nickel layer onto the Pd nanosprings leads to tiny magnetic helical nanoswimmers (as small as 100 nm in diameter and 600 nm in length) (Fig. 1e). Applying a continuous torque to the new Ni-coated Pd nanohelices, *via* a rotating magnetic field, transforms the rotation around their helical axis into a translational corkscrew motion along this axis.

We initially used AAO membrane templates with pore diameter of ~200 nm for preparing the helical nanoswimmers. Stepwise schematic illustrations and SEM images of the nanostructures prepared at the different steps of the synthesis are displayed in Fig. 2a–c. For example, the SEM image of Fig. 2a depicts the surface morphology of a Pd/Cu alloy nanorod released during the NaOH-induced dissolution of AAO membrane. A close examination of this image indicates the presence of periodical helical dented curvature on the nanorod surface, corresponding to Pd nanodomains curling up on the Cu nanorod, and reflecting the coiled-shaped growth of Pd.[32] Subsequent 10 min exposure of this Pd/Cu rod structure to an 8 M nitric acid solution results in etching of the Cu component, leaving behind a helical Pd nanospring structure with a rough surface (SEM image of Fig. 2b). Longer etching time can damage (slowly dissolve) the Pd nanospring structures. While the exact reason for the formation of the Pd nanospring is not fully understood, it has been attributed to the spatially different growth processes of Pd and Cu.[32] The circular cross section of the filament of this helical Pd nanostructure has a diameter of about 40 nm. A smoother surface is observed Fig. 2c after the electron beam evaporation of a uniform and thin Ni film over the Pd nanohelix. In order to improve the coating uniformity, the deposition rate of the Ni layer was maintained as low as 0.05 nm s^{-1} under a very low pressure (10^{-7} torr).

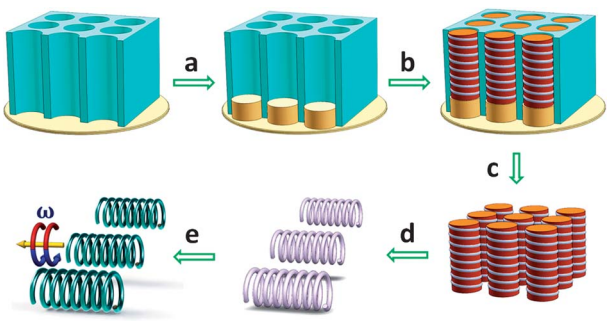

Fig. 1 Schematic illustration of the template-based fabrication of helical magnetic nanoswimmers. (a) Electrodeposition of Au; (b) electrochemical codeposition of Pd/Cu rods; (c) removal of the membrane template and the Au bottom layer; (d) etching of Cu; (e) Ni coating for magnetic actuation.

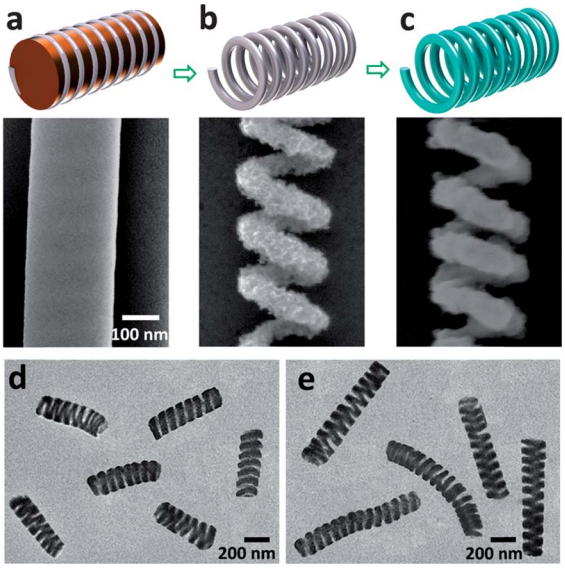

Fig. 2 Schematic and SEM images of a Pd/Cu nanorod (showing periodical helical indented curvature on the surface) (a), the Pd helical nanospring (b) and the Ni-coated Pd helical nanospring (c). (d and e) TEM characterization of magnetic nanohelices of different lengths: ~800 nm (d) and ~1.5 μm (e), prepared using charge densities of 0.5 and 1 C cm^{-2}, respectively.

The template electrosynthesis method can produce helical nanopropellers with tailored-made geometries and dimensions. For example, controlling the charge density during the Pd/Cu deposition has been used for producing nanohelices with different lengths. The transmission electron microscopy (TEM) images of Fig. 2d show well-defined nanohelices with a length of around 800 nm, prepared using a charge density of 0.5 C cm^{-2}. Increasing the charge density to 1 C cm^{-2} results in longer helices with an average length of ~1.5 μm, (Fig. 2e). It should be noted that nanosprings with aspect ratios larger than 15 display some bending and may compromise the magnetic locomotion. Nanohelices with aspect ratios smaller than 10 were thus used for most subsequent propulsion experiments.

Another attractive feature of the new template electrosynthesis route is its ability to tailor the helical pitch through control of the composition of plating solution. In particular, the morphology of the helices is strongly dependent on the Pd^{2+}/Cu^{2+} concentration ratio in the solution. The absence of copper in the solution leads to the formation of Pd nanotubes due to the higher Pd^{2+} reduction rate at the surface of the nanopore.[32] Similarly, the helical architecture is not observed using plating solutions with very high Cu^{2+} concentrations, since such solutions hinder the nanohelix growth and lead to highly porous Pd nanorods.[32] In order to tailor the helical pitch of the resulting nanohelices, we thus used plating solutions with a Cu^{2+} concentration of 20 mM and Pd^{2+} concentrations ranging from 25 mM to 45 mM. Fig. 3a–e displays a series of SEM images of nanohelices prepared with varied Pd^{2+} concentrations: (a) 25, (b) 30, (c) 35, (d) 40 and (e) 45 mM. Fig. 3f summarizes the observed effect of the composition of the plating solution and shows the dependence of the helical pitch length upon the Pd^{2+}/Cu^{2+} concentration ratio. These data and images indicate that the pitch length decreases gradually from ~130 nm to ~60 nm upon increasing the Pd^{2+} concentration from 20 mM to 45 mM. The resultant structure finally approaches a nanotube at the highest Pd^{2+} level. Overall, a plating solution containing 30 mM $PdCl_2$, 20 mM $CuCl_2$, and 0.1 M HCl is optimal for preparing well-defined Pd nanosprings towards efficient helical magnetic nanoswimmers.

The electrodeposition strategy allows precise control of the diameter of helical Pd nanostructure, and of the corresponding nanoswimmers, through the use of membrane templates with different pore sizes. Since commercial Polycarbonate (PC) membranes have a larger variety of pore diameters (ranging from 15 nm to 12 μm) than AAO templates, it is possible to use different PC membrane templates for preparing helical nanoswimmers with different diameters. Accordingly, we evaluated polycarbonate membranes with pore diameters of 100 nm and 400 nm (along with the AAO membrane with 200 nm pores). Since hydroxyl (OH) group-terminated alumina surfaces in acidic environment are critical for nanohelix formation due to the interfacial electrostatic double layer formation in nanochannels,[32] we used atomic layer deposition (ALD) for incorporating alumina into walls of the PC membrane micropores. Electrodeposition of Pd/Cu alloy nanorods has been subsequently carried out under the optimal conditions (30 mM $PdCl_2$/20 mM $CuCl_2$), followed by dissolution of the PC template and the Cu component using methylene chloride and 8 M nitric acid, respectively. ESI Fig. 1† displays long Pd nanosprings encapsulated within 400 nm diameter Al_2O_3 nanotubes after the dissolution of the PC membrane. Subsequent NaOH-induced dissolution of the Al_2O_3 nanotubes and electron beam evaporation of Ni layer resulted in the formation of magnetic helical nanoswimmers of different diameters. Fig. 4 displays a series of SEM and TEM images of such magnetic nanohelices formed inside nanopores of varying diameters. These images indicate that well-defined nanohelices of diameters ranging from 100 to 400 nm can be prepared using membrane templates possessing

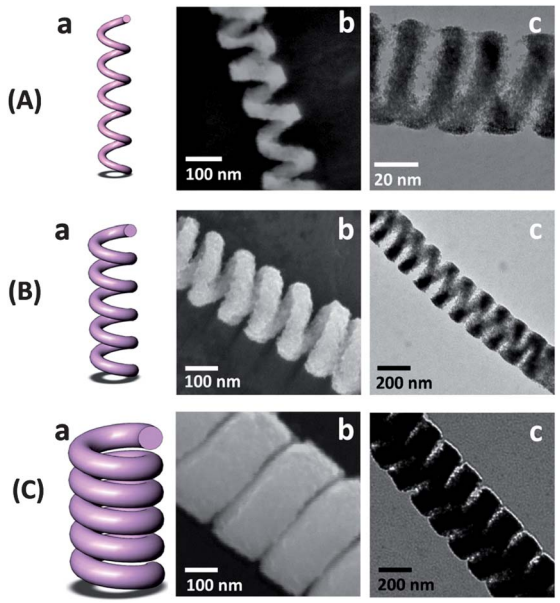

Fig. 4 Schematic illustrations (a), SEM (b) and TEM (c) images of Ni/Pd nanohelices with different diameters: 100 (A), 200 (B) and 400 (C) nm prepared by using different membrane templates.

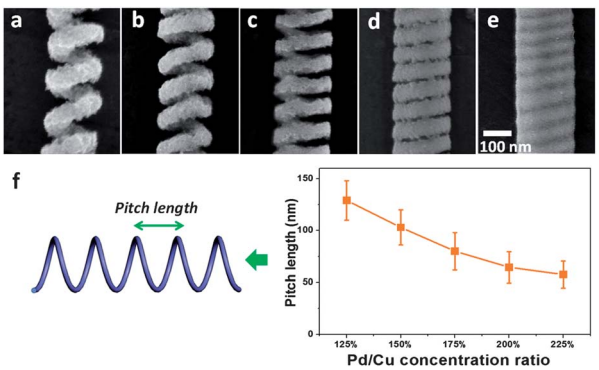

Fig. 3 Control of the pitch length of the template-prepared magnetic nanohelices. (a–e) SEM images of Ni–Pd nanosprings. $PdCl^{2+}$/$CuCl^{2+}$ concentration ratio in the plating solution: (a) 25/20, (b) 30/20, (c) 35/20, (d) 40/20, (e) 45/20. (f) Plot showing the dependence of the pitch length upon the Pd^{2+}/Cu^{2+} concentration ratio.

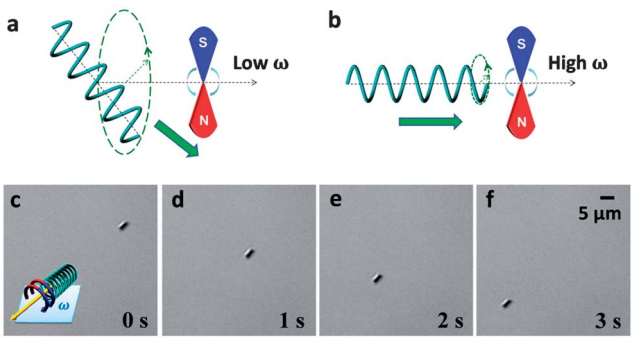

Fig. 5 Schematic illustration of the tumbling (a) and corkscrew (b) motions of helical nanoswimmer under low and high magnetic rotation frequencies, respectively. (c–f) Time-lapse motion images (taken from ESI Video S2†) of a 400 nm helical nanoswimmer under a magnetic rotation frequency of 150 Hz.

nanopores of different diameters. Note also that the cross section of the filament increases from ~30 nm to ~150 nm upon increasing the diameter of the nanopores.

Following the successful template fabrication of tailored-made magnetic nanohelices, a rotating magnetic field has been used to remotely actuate their directional motion. The new template-prepared torque-driven nanoswimmers display an attractive propulsion behavior: tumbling motion at low magnetic rotation frequency and corkscrew motion at high magnetic rotation frequencies (Fig. 5a and b, respectively).[6,19] The change from tumbling to a corkscrew rotation occurs at a specific stabilization frequency. Such frequency-dependent transition motion behavior is illustrated in ESI Video S1† for a 400 nm diameter helical nanoswimmer, upon increasing the magnetic field frequency from 10 to 100 Hz. Subsequent work has focused on the corkscrew motion of the new template-prepared nanoswimmers. The image sequence of Fig. 5c–f (taken from ESI Video S2†) displays such movement using a 3 μm long (400 nm diameter) nanoswimmer over the 3 s period at a rotation frequency of 150 Hz. The nanoswimmer travels over a long path of approximately 45 μm parallel to the magnetic field axis, *i.e.*, at a speed of 15 μm s^{-1}, corresponding to a relative speed of ~5 body lengths s^{-1}. Such speed compares favorably with those reported for helical swimmers prepared by advanced self-scrolling and GLAD techniques.[16,21,22] The new helical swimmers also displayed effective propulsion in cell culture media, which is in agreement with a previous study of the magnetic nanoswimmers in salt-rich media.[18]

The translational velocity of helical nanoswimmers with different diameters has been examined using different magnetic rotation frequencies. The trajectories in Fig. 6a–c illustrate the (taken from ESI Video S3†) defined motion of different helical nanoswimmers with diameters of 100, 200 and 400 nm, respectively, over a 2 second period at a rotation frequency of 120 Hz. Tracking analysis demonstrates that their average speeds are 6, 9 and 13 μm s^{-1}, respectively. The influence of the frequency upon the speed of helical nanoswimmers of different diameters is shown in Fig. 6d. These plots indicate that the motor speed increases in a nearly linear fashion with the frequency. Furthermore, it is noted that large nanoswimmers (with a 400 nm diameter) swim nearly 3-fold faster than the smaller (100 nm) ones. The speed of helical swimmers is dependent upon various geometric parameters (including the diameter) and the rotation frequency, in a complex manner described in eqn (1):[23,33]

$$v = \frac{(\xi_{\perp} - \xi_{\parallel})\sin\theta\ \cos\theta}{2(\xi_{\perp}\sin^2\theta + \xi_{\parallel}\cos^2\theta)} d\omega \quad (1)$$

where $\xi_{\perp}$ and $\xi_{||}$ are the drag coefficients perpendicular and parallel to the helical axis, θ is the helix angle, d is diameter of the helix, and ω is the rotational frequency. Overall, our experimental results follow closely the theoretical prediction of equation.

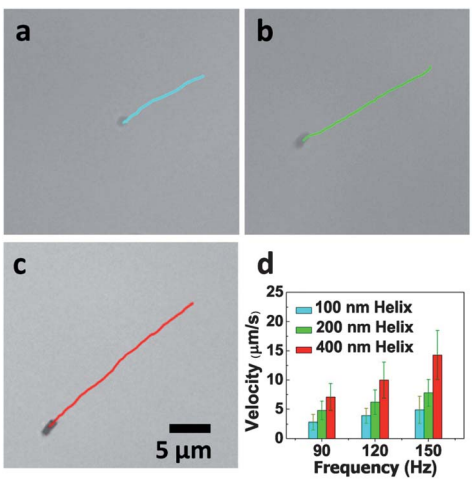

Fig. 6 Motion trajectories of helical nanoswimmers with different diameters: (a) 100 nm; (b) 200 nm; (c) 400 nm (aspect ratios of ~10) over a 2 s period. Magnetic field frequency: 120 Hz. (d) Dependence of the nanoswimmer velocity on the magnetic frequency and diameter of the motors, calculated from the tracking analysis of the observed motion.

Conclusions

In summary, we have demonstrated an attractive template-electrosynthesis approach for the fabrication of the extremely small yet highly efficient helical magnetic nanoswimmers. The Pd helical nanostructures were fabricated by template electrodeposition of Pd/Cu nanorods into nanoporous membrane templates, followed by removal of Cu, and electron-beam coating the resulting Pd nanohelices with a magnetic Ni layer. The new templating route results extremely small (of 100 nm diameter) and efficient helical nanoswimmers and allows convenient tailoring of the length, diameter and helix pitch of nanohelices. These template-prepared fuel-free helical nanoswimmers display an attractive locomotion behavior and are promising for a plethora of future biomedical applications, such as *in vivo* targeted drug delivery or biopsy.

Experimental section

1. Synthesis of magnetic nanohelices

Nanoporous AAO membranes (6809-6022, Whatman, Maidstone, UK) with a pore size of 200 nm were used as a template for fabricating 200 nm nanohelices. PC membrane templates (110605 and 110607, Whatman, NJ, USA) with pore sizes of 100 nm and 400 nm were used for fabricating 100 and 400 nm helical nanoswimmers. Al_2O_3 coatings were formed in the PC templates by atomic layer deposition for 800 cycles at 100 °C. Before electrochemical deposition, a 75 nm gold film was sputtered on one side of the porous membrane to serve as a working electrode using the Denton Discovery 18 (Moorestown, NJ). A Pt wire and an Ag/AgCl (with 1 M KCl) were used as counter and reference electrodes, respectively. The membrane was then assembled in a plating cell with an aluminium foil serving as a contact. All electrochemical deposition steps were carried out at room temperature (22 °C). For preparing 200 nm nanohelices using an AAO membrane, a sacrificial silver layer

was initially electrodeposited at −1.0 V for a total charge of 3C using a commercial silver plating solution (1025 RTU @ 4.5 Troy/gallon). Gold nanorods were then electrodeposited at −1.0 V for a total charge of 1.5C from a commercial gold plating solution (Orotemp 24 RTU RACK); subsequently, the Pd/Cu nanorods were deposited at −0.1 V from the $PdCl_2/CuCl_2$ plating solution mixture. All the Pd/Cu plating solutions contained 20 mM $CuCl_2$ and 0.1 M HCl, while the $PdCl_2$ concentrations varied from 25 mM to 45 mM to prepare nanohelices with different morphologies. After electrochemical deposition, the sputtered gold layer was completely removed by hand polishing with 3–4 μm alumina slurry. The AAO membrane templates were dissolved in 3 M NaOH for 30 min followed by washing with ultrapure water until neutral pH was obtained. Finally, the Ag sacrificial layer and the Cu component (of the Pd/Cu nanorods) were dissolved using an 8 M HNO_3 solution for 10 minutes, resulting in the formation of Pd nanohelices. Fabrication of 100 nm and 400 nm nanohelices, with the PC membrane templates involved the electrodeposition of gold nanorods using a charge of 0.2C; and subsequent deposition of Pd/Cu nanorods at −0.1 V from a plating solution containing 20 mM $CuCl_2$, 30 mM $PdCl_2$ and 0.1 M HCl for 2C. The templates were dissolved in methylene chloride for 10 min to completely release the nanostructures. The latter were collected by centrifugation at 9000 rpm for 3 min and washed 3 times with methylene chloride, ethanol and deionized water each, with a 3 min centrifugation after each wash. Finally, Pd/Cu nanorods were soaked in a NaOH (3 M) solution for 30 min to dissolve Al_2O_3 for a complete release of nanorods. The Cu in the Pd/Cu nanorods was then etched as mentioned above. The Pd nanohelices were dispersed on glass slides. Finally, a 10 nm thick Ni layer was deposited onto the Pd nanohelices by electron beam evaporation, using a deposition speed of 0.05 nm s^{-1}.

2. Magnetic actuation and microscopy observation

A Helmholtz coil pair was used to generate the magnetic rotation field for remote actuation. The frequency of the rotating magnetic field can be changed from 1 Hz to 1000 Hz by a sinusoidal wave generator. The above magnetic nanohelices were dispersed in water droplets for rotation and translation motion tests. An inverted optical microscope (Nikon Instrument Inc. Ti-S/L100), coupled to a 40 ×objective, a Hamamatsu digital camera C11440 and NIS Elements AR 3.2 software, were used for capturing movies of the swimming motion. The speed of the nanoswimmers was tracked using a NIS Elements tracking module.

Acknowledgements

This project was supported from the Defense Threat Reduction Agency–Joint Science and Technology Office for Chemical and Biological Defense (Grant no. HDTRA1-13-1-0002). R. D. acknowledges financial support from the China Scholarship Council (CSC). W. G. is a HHMI International Student Research fellow. The authors thank C. R. Kane, D. Wiitala, and M. J. Galarnyk for their assistance.

Notes and references

1 J. Wang, *Nanomachines: Fundamentals and Applications*, Wiley-VCH, Weinheim, Germany, 2013, ISBN 978-3-527-33120-8.
2 T. E. Mallouk and A. Sen, *Sci. Am.*, 2009, **300**, 72.
3 G. A. Ozin, I. Manners, S. Fournier-Bidoz and A. Arsenault, *Adv. Mater.*, 2005, **17**, 3011.
4 J. Wang and W. Gao, *ACS Nano*, 2012, **6**, 5745.
5 Y. F. Mei, A. A. Solovev, S. Sanchez and O. G. Schmidt, *Chem. Soc. Rev.*, 2011, **40**, 2109.
6 B. J. Nelson, I. K. Kaliakatsos and J. J. Abbott, *Annu. Rev. Biomed. Eng.*, 2010, **12**, 55.
7 W. F. Paxton, K. C. Kistler, C. C. Olmeda, A. Sen, S. K. St Angelo, Y. Y. Cao, T. E. Mallouk, P. E. Lammert and V. H. Crespi, *J. Am. Chem. Soc.*, 2004, **126**, 13424.
8 W. Gao, S. Sattayasamitsathit, J. Orozco and J. Wang, *J. Am. Chem. Soc.*, 2011, **133**, 11862.
9 J. X. Li, J. Zhang, W. Gao, G. S. Huang, Z. Di, R. Liu, J. Wang and Y. F. Mei, *Adv. Mater.*, 2013, **25**, 3715.
10 G. Loget and A. Kuhn, *J. Am. Chem. Soc.*, 2010, **132**, 15918.
11 S. T. Chang, V. N. Paunov, D. N. Petsev and O. D. Velev, *Nat. Mater.*, 2007, **6**, 235.
12 M. Liu, T. Zentgraf, Y. M. Liu, G. Bartal and X. Zhang, *Nat. Nanotechnol.*, 2010, **5**, 570.
13 W. Wang, L. A. Castro, M. Hoyos and T. E. Mallouk, *ACS Nano*, 2012, **6**, 6122.
14 D. Kagan, M. J. Benchimol, J. C. Claussen, E. Chuluun-Erdene, S. Esener and J. Wang, *Angew. Chem., Int. Ed.*, 2012, **124**, 7637.
15 R. Dreyfus, J. Baudry, M. L. Roper, M. Fermigier, H. A. Stone and J. Bibette, *Nature*, 2005, **437**, 862.
16 L. Zhang, J. J. Abbott, L. X. Dong, B. E. Kratochvil, D. Bell and B. J. Nelson, *Appl. Phys. Lett.*, 2009, **94**, 064107.
17 P. Fischer and A. Ghosh, *Nanoscale*, 2011, **3**, 557.
18 W. Gao, S. Sattayasamitsathit, K. M. Manesh, D. Weihs and J. Wang, *J. Am. Chem. Soc.*, 2010, **132**, 14403.
19 K. E. Peyer, S. Tottori, F. Qiu, L. Zhang and B. J. Nelson, *Chem.–Eur. J.*, 2013, **19**, 28.
20 H. C. Berg and R. A. Anderson, *Nature*, 1973, **245**, 380.
21 D. J. Bell, S. Leutenegger, K. M. Hammar, L. X. Dong and B. J. Nelson, *IEEE Int. Conf. Robot. Autom.*, 2007, 1128.
22 A. Ghosh and P. Fischer, *Nano Lett.*, 2009, **9**, 2243.
23 S. Tottori, L. Zhang, F. M. Qiu, K. K. Krawczyk, A. Franco-Obregon and B. J. Nelson, *Adv. Mater.*, 2012, **24**, 811.
24 S. Kim, F. Qiu, S. Kim, A. Ghanbari, C. Moon, L. Zhang, B. J. Nelson and H. Choi, *Adv. Mater.*, 2013, DOI: 10.1002/adma.201301484.
25 Y. D. Liu, J. Goebl and Y. D. Yin, *Chem. Soc. Rev.*, 2013, **42**, 2610.
26 C. R. Martin, *Chem. Mater.*, 1996, **8**, 1736.
27 J. Wang, *Faraday Discuss.*, 2013, DOI: 10.1039/c3fd00105a.
28 T. R. Kline, W. F. Paxton, T. E. Mallouk and A. Sen, *Angew. Chem., Int. Ed.*, 2005, **44**, 744.
29 G. S. Huang, J. Wang and Y. F. Mei, *J. Mater. Chem.*, 2012, **22**, 6519.

30 G. J. Zhao and M. Pumera, *RSC. Adv.*, 2013, **3**, 3963.
31 Y. Y. Wu, G. S. Cheng, K. Katsov, S. W. Sides, J. F. Wang, J. Tang, G. H. Fredrickson, M. Moskovits and G. D. Stucky, *Nat. Mater.*, 2004, **3**, 816.
32 L. Liu, S. H. Yoo, S. A. Lee and S. Park, *Nano Lett.*, 2011, **11**, 3979.
33 E. Lauga and T. R. Powers, *Rep. Prog. Phys.*, 2009, **72**, 096601.